ISBN: 978-3-95450-184-7 doi:10.18429/JACoW-IPAC2018-THPML129

DEPOSITION AND CHARACTERIZATION OF TIZRHFV FILMS BY DC MAGNETRON SPUTTERING#

Xiaoqin Ge, Yigang Wang, Yuxin Zhang, Tianlong He, Bo Zhang*, Xiangtao Pei, Wei Wei and Yong Wang*
NSRL, USTC, Hefei, Anhui 230029, China

Abstract

The new generation of accelerators places higher demands on the surfaces of vacuum chamber materials. Search for low secondary electron yield (SEY) materials and an effective vacuum chamber surface treatment process, which can effectively reduce the electronic cloud effect, are important early works for the new generation of accelerators. In this work, we revealed the SEY characteristics of Ti-Zr-Hf-V NEG films and Ti-Zr-V NEG films which were deposited on Si (111) substrates using direct current magnetron sputtering method. The surface morphology and surface chemical bonding information were collected by scanning electron microscopy (SEM) and X-ray photoelectron spectroscopy (XPS). With the same parameters, the maximum SEY of Ti-Zr-Hf-V NEG films and Ti-Zr-V NEG films are 1.24 and 1.51, respectively. These results are of great significance for the next-generation particle accelerators.

INTRODUCTION

It's noteworthy that the residual gas in the vacuum chamber will cause the loss of the beam in high-energy particle accelerators, which requires minimizing the residual gas in the vacuum chamber to ensure a higher ultimate vacuum degree. Therefore, the most direct method to increase the ultimate vacuum is to perform certain surface treatments on the inner wall to reduce the surface deflation. Thus, coating a non-evaporable getter (NEG) [1-5] film on the surface of inner wall for storage ring is an effective way to improve the vacuum degree.

In recent years, many laboratories have conducted long-term and in-depth systematic studies on the secondary electron emission of storage ring vacuum chamber materials during accelerator design and construction, such as CESR [6], SLAC [7], Fermilab [8, 9], NSRL and many more. High quality beam current is one of the main goals in the design and fabrication of new accelerators. However, under a large number of scattering particle bombardment collisions, secondary electrons excited on the surface of the storage ring vacuum chamber will form an electron cloud, which will affect beam quality (including beam stability, energy, emission and life). Therefore, it is crucial to find a stable and very low SEY materials for future high-intensity accelerators [10-12].

In this article, the Ti-Zr-Hf-V and Ti-Zr-V NEG films were fabricated on the Si (111) substrates. The morphology and surface information are characterized. The SEY of this films are further investigated to understand the inhalation performance.

EXPERIMENT

Coating System and Methods

The quaternary Ti-Zr-Hf-V coating with a lower activation temperature has been fabricated through direct current (DC) magnetron sputtering. The DC magnetron sputtering coating system is showed in Fig. 1 with a stainless steel pipe to be plated.

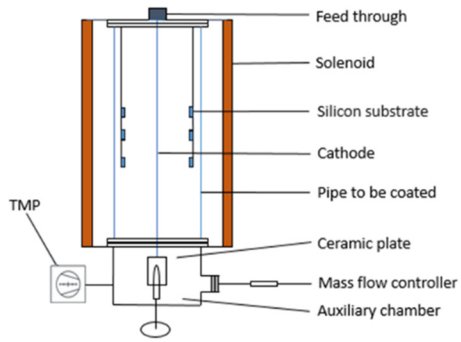

Figure 1: DC magnetron sputtering coating system.

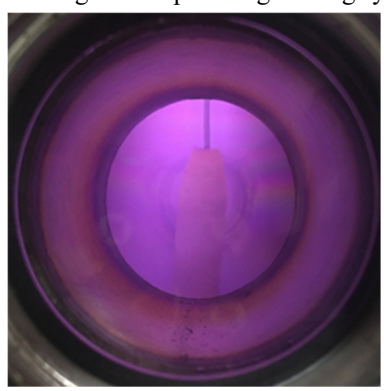

Figure 2: Glow discharge.

The cathode target is made of four twisted metal wires (Ti, Zr, Hf and V) with a diameter of 2 mm and purity of 99.9%, 99.5%, 99.5%, and 99.5%, respectively. The end of the cathode target is equipped with a ceramic chip to ensure insulation from the inner wall of the pipe. Firstly, the cleaned sample was put into the pipe to be plated before coating. Then, the residual gas in the system was eliminated by pumping and baking the pipe. The Kr flow was introduced under the control of flow controller after the limit pressure was reached. Kr gas has higher stability than Ar gas commonly used in coating. When the air

#Work supported by the National Nature Science Foundation of China under Grant Nos. 11475166
* zhbo@ustc.edu.cn, ywang@ustc.edu.cn

ISBN: 978-3-95450-184-7 doi:10.18429/JACoW-IPAC2018-THPML129

pressure reaches the glow discharge zone, the solenoid coil power supply and discharge power supply are sequentially turned on to start the DC magnetron sputtering. The resulting glow discharge is shown in Fig. 2.

The deposition rate of the film is mainly determined by the power density of the discharge. Generally, the higher power density can introduce the higher deposition rate. We estimate the deposition rate based on a number of experimental experiences to determine the coating time. The parameters such as discharge current and air pressure can be adjusted to ensure stable discharge during the coating process. Typical coating parameters for this experiment are shown in Table 1. The Ti-Zr-V NEG film production process is exactly the same except that the Hf wire is taken out.

Table 1: Coating Parameters

Parameter	Value
Coating time	8 h
Discharge current	0.3 A
Magnetic field strength	200 G
Working pressure	2 Pa
Cathode voltage	-500 V

SEY Measurement

The device for testing SEY used in this paper is mainly composed of five parts: vacuum system, test system, control system, data acquisition and processing system. The vacuum system is used to provide the sealed vacuum environment required for secondary electron emission and is the most basic framework of the entire tester. The test system mainly realizes the generation of incident electrons and the output of SEY signals, and is the most central part of the entire tester. The control and data acquisition system is used to measure the secondary electron current signal and control the parameters of the incident electron beam.

The material secondary electron characteristic parameter tester adopts Kimball Physics EGL-2022 electron gun, and the incident electron beam hits the sample vertically. In the ECC mode, the energy range of the incident electron beam is 50 eV to 5000 eV. The current signal was collected using a Keithley 2400 picoammeter with an accuracy of 0.012%. During the test, the vacuum chamber is grounded with a chamber vacuum of 10^{-7} Pa under 300K. The SEY test method is shown in Eq. (1). The SEY measurement method is shown in Fig. 3.

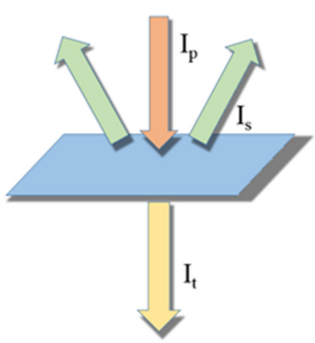

Figure 3: The schematic diagram of SEY measurement.

$$I_{SEY} = \frac{I_{SEY}}{I_p} = 1 - \frac{I_t}{I_p} \quad (1)$$

RESULTS AND DISCUSSION

Film Properties

Figure 4 is a cross-sectional view of a Ti-Zr-Hf-V film obtained by SEM. The thickness is 1.63μm while the thickness of the Ti-Zr-V film is 1.71μm under the same parameters, indicating that the coating efficiency of Ti-Zr-Hf-V is as better as that of Ti-Zr-V. The fibrous structure shown in Fig. 4 is easily formed because the deposited atoms do not have a strong diffusion ability on the surface of the substrate and mainly diffuse on the surface of the film and the grain boundary under a low deposition temperature. The nucleation rate on the substrate is faster under a faster film deposition rates. Furthermore, sputtered target atoms have less loss due to gas scattering at low operating pressures, thus it is easy to obtain a very dense fibrous structure of the film.

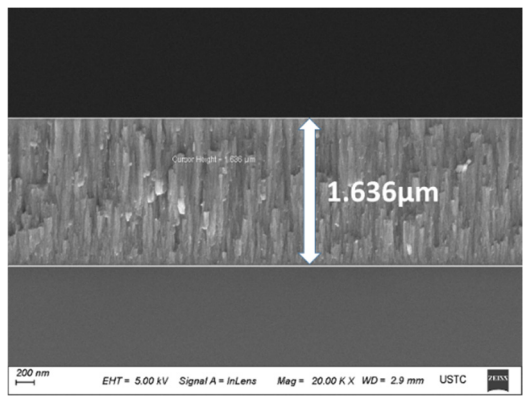

Figure 4: Cross section of the Ti-Zr-Hf-V film obtained by SEM.

Figure 5 shows the surface morphology information of the thin film obtained by SEM. It can be seen that the surface is composed of many fine particles. The pores between these particles can be seen as a container for storing gas. After the active gas molecules enter these pores, they are likely to be adsorbed on its surface.

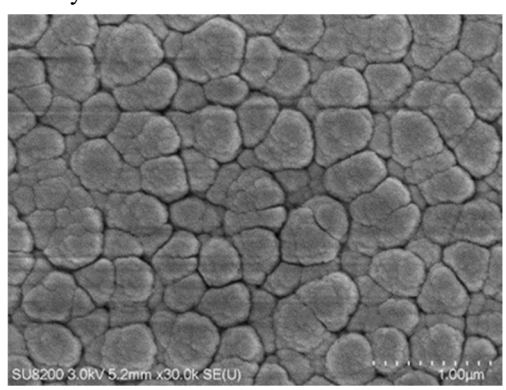

Figure 5: Surface Observation of the Ti-Zr-Hf-V film obtained by SEM.

The full spectrum of XPS is shown in Fig. 6. The composition ratio of each element is calculated based on

ISBN: 978-3-95450-184-7 doi:10.18429/JACoW-IPAC2018-THPML129

the whole spectrum, as shown in Table 2. We can conclude that the ratio of the three elements in the Ti-Zr-V film is close to 1:1:1. However, in the Ti-Zr-Hf-V thin film, the sputtering efficiency of Hf is far greater than that of the other three elements. This may be due to the fact that the Hf wire has a shorter residence time than the other three wires and is less oxidized. XPS has a depth of detection of a few nanometers and is generally not detectable below the passivation layer. The measurement results revealed the composition of the components in the passivation layer and thus large amount of oxygen and carbon could be observed.

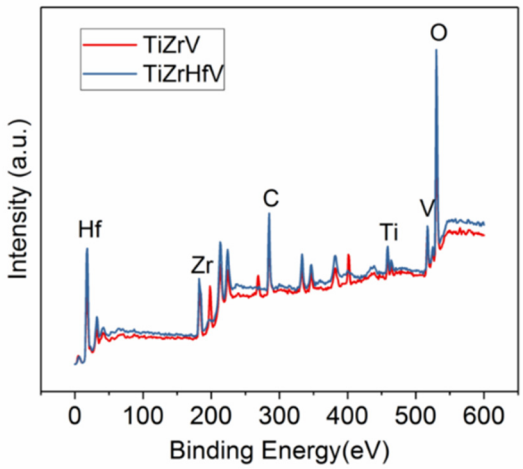

Figure 6: The full spectrum of XPS.

Table 2: Film Composition Ratio Measured by XPS

	Ti	Zr	V	Hf	O	C
TiZrV	3.88	4.21	4.9	-	46.12	40.89
TiZrHfV	2.96	4.28	3.8	7.66	43.55	37.75

SEY

Figure. 7 shows that the I_{max} of Ti-Zr-Hf-V films and Ti-Zr-V films are 1.24 and 1.51 respectively. It can be seen that Ti-Zr-Hf-V film here greatly reduces the SEY. This phenomenon may be due to the difference in the microstructure of the two films, and the exact cause remains to be seen.

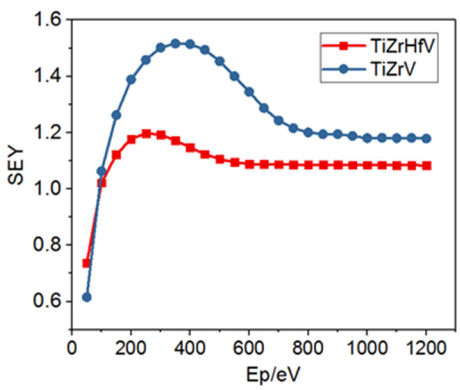

Figure 7: SEY of Ti-Zr-Hf-V films and Ti-Zr-V films.

CONCLUSION

In summary, we firstly demonstrated the new Ti-Zr-Hf-V NEG films on the Si (111) substrates through DC magnetron sputtering method. This new formed quaternary alloy NEG film showed ideal performance with a low initial TEY. Benefit from the easy fabrication method and low activation temperature of Ti-Zr-Hf-V NEG films, the Ti-Zr-Hf-V NEG films could be a candidate for modern particle accelerators.

REFERENCES

[1] P. Chiggiato et al., "Ti–Zr–V non-evaporable getter films: From development to large scale production for the Large Hadron Collider", *Thin Solid Films*, vol. 515, pp. 382-388, 2006. doi: 10.1016/j.tsf.2005.12.218

[2] O. B. Malyshev et al., "Pumping properties of Ti–Zr–Hf–V non-evaporable getter coating", *Vacuum,* vol. 100, pp. 26-28, 2014. doi:10.1016/j.vacuum.2013.07.035

[3] J. Setina et al., "Measuring volume ratios of vacuum vessels using non-evaporable getters", *Vacuum*, vol. 92, pp. 20-25, 2013. doi: 10.1016/j.vacuum.2012.11.010

[4] C. Benvenuti et al., "Decreasing surface outgassing by thin film getter coatings", *Vacuum*, vol. 50, pp. 57-63, 1998. doi: 10.1016/S0042-207X(98)00017-7

[5] C. Benvenuti et al., "Vacuum properties of TiZrV non-evaporable getter films", *Vacuum*, vol. 60, pp. 57-65, 2001. doi: 10.1016/S0042-207X(00)00246-3

[6] W. Hartung et a.l, "Measurements of secondary electron yield of metal surfaces and films with exposure to a realistic accelerator environment", in *Proc. IPAC2013*, Shanghai, China, Jun. 2013, pp. 3493-3495.

[7] R. E. Kirby et al., "Secondary electron emission yields from PEP-II accelerator materials", *Nuclear Instruments and Methods in Physics Research Section A: Accelerators, Spectrometers, Detectors and Associated Equipment*, vol. 469, pp. 1-12, 2001. doi: 10.1016/S0168-9002(01)00704-5

[8] D. J. Scott et al., "Secondary electron yield measurements of fermilab's main injector vacuum vessel", in *Proc. IPAC2012*, New Orleans, Louisiana, USA, May 2012, paper MOPPC019, pp.166-168.

[9] Y. Ji et al., "Secondary electron yield measurement and electron cloud simulation at Fermilab", in *proc. IPAC2015*, Richmond, VA, USA, Jun 2015, paper MOPMA039 pp. 629-632.

[10] Y. Suetsugu et a.l, "Results and problems in the construction phase of the SuperKEKB vacuum system", *Journal of Vacuum Science & Technology A: Vacuum, Surfaces, and Films*, vol. 34, pp. 021605, 2016, doi: 10.1116/1.4942455

[11] R. Cimino et al., "Search for new e-cloud mitigator materials for high intensity particle accelerators" *in proc. IPAC2014*, Dresden, Germany, Jun 2014, pp.WEPME033, pp. 2332-2334.

[12] C. Garion et al., "Material characterisation and preliminary mechanical design for the HL-LHC shielded beam screens operating at cryogenic temperatures", *IOP Conf. Series: Materials Science and Engineering*, vol. 102, pp. 012013, 2015.